J. exp. Biol. ***193****, 97–117 (1994)*
Printed in Great Britain © The Company of Biologists Limited 1994

ION TRANSPORT IN THE INTESTINE OF *ANGUILLA ANGUILLA*: GRADIENTS AND TRANSLOCATORS

P. MARVÃO, M. G. EMÍLIO, K. GIL FERREIRA*, P. L. FERNANDES AND H. GIL FERREIRA

Laboratory of Physiology, Gulbenkian Institute of Science, Oeiras, Portugal

Accepted 19 April 1994

Summary

The transport of Na^+, K^+ and Cl^- across the isolated epithelium of the eel intestine was studied using a combination of four experimental strategies: short-circuiting, measurements of intracellular potentials and ion concentrations, application of a variety of transport inhibitors and measurement of unidirectional fluxes with radioactive tracers. When short-circuited, the system performs a net transport of Cl^- and Na^+ towards the blood side, with a stoichiometry approaching 2, and a much smaller net transport of K^+ towards the lumen. The system is totally driven by the sodium pump located in the basolateral barrier and the main coupling between the fluxes of the three ions is through the operation of a furosemide-sensitive transporter in the apical barrier, probably a $2Cl^-/Na^+/K^+$ symporter. The inhibitory effect of DIDS and picrylsulphonic acid on the short-circuit current, when added to the serosal side, suggests the presence of a sodium-dependent anionic shuttle located in the basolateral membrane. The short-circuit current is inhibited by H25, a non-specific inhibitor of the K^+/Cl^- symport, added to the serosal side. This effect occurs after a delay of at least 5 min and may result from the diffusion of the drug to the apical barrier, where it blocks the $2Cl^-/Na^+/K^+$ symport with much higher affinity.

Introduction

The intestine of salt-adapted eels performs a vigorous coupled transport of water and NaCl. This coupling was initially reported, under open-circuit and in *in vitro* perfused preparations by Ando *et al.* (1974), who showed that, after salt-adaptation, there was uphill transport of sodium, chloride and water towards the serosal (blood) side together with increases in the unidirectional fluxes of sodium and chloride and in the osmotic permeability. Under the same conditions, sodium was transported at the same rate as chloride. The water transport correlated very well with the transepithelial electrical potential difference and depended on external chloride concentration above 50 mmol l^{-1} (Ando, 1975). Ion substitution experiments showed a tight dependence of the water and sodium transport on chloride (Ando, 1980) and measurements of open-circuit potentials

*To whom reprint requests should be addressed.

Key words: ion transport, transport inhibitors, intestine, eel, *Anguilla anguilla*.

in chloride-free solutions suggested the presence of a sodium pump, later confirmed by the effect of ouabain on the water transport and on the open-circuit potential (Ando, 1981). Simultaneous measurements of net sodium, potassium, chloride and water fluxes, in the presence and absence of chloride in the external solutions and in the presence of ouabain, indicated that the four fluxes were tightly coupled (Ando, 1983, 1985), as previously shown by Field *et al.* (1978) and Musch *et al.* (1982) for the flounder intestine in relation to sodium, potassium and chloride fluxes. The model initially proposed for the flounder intestine and based on these observations (see Palfrey and Rao, 1983) was subsequently adopted by Ando and Utida (1986) for the eel intestine. It included $2Cl^-/Na^+/K^+$ symport at the apical barrier and a sodium pump together with Cl^-/K^+ symport at the basolateral barrier. The suggestion for the presence of this transporter was based on the inhibitory effect on water transport of replacing sodium by potassium in the serosal bath (Ando, 1983). The bicarbonate-dependence of the chloride transport, later reported by Ando (1990) and by Schettino *et al.* (1992), was not included in this model. Almost all of this work was performed on *Anguilla japonica*, in general under open-circuit conditions, which are nearer to the physiological situation but less easy to analyze because of the electrical coupling between the ion fluxes through the transepithelial electrical potential. Ideally, the identified transporters should be seen as being components of an integrated transport system which performs the transepithelial transport of ions and water. The construction of a model of such a system entails the characterization of the ionic electrochemical gradients across the apical and basolateral barriers and identification of the translocated species. In this paper, we aimed to gather data which will ultimately enable us to make a complete and quantitative description of the system. This entailed the partial repetition of some published experiments, in particular by Ando and his co-workers, although under different experimental conditions, namely under short-circuiting conditions. For the first time, intracellular electrical potentials and ion concentrations, measured with double-barrelled ion-sensitive microelectrodes, and the effects of a variety of transport inhibitors and fluxes, measured with radioisotope tracers, are presented.

Materials and methods

Eels (*Anguilla anguilla* L.) weighing 80–350 g, freshly collected (less than 1 week earlier) in the mouth of the river Tagus, were kept in a freshwater aquarium. Animals were killed by decapitation and pithing. The posterior intestine was excised through a mid-abdominal incision and a fire-polished glass rod 4 mm in diameter was inserted into the lumen. The upper extremity was tied onto the rod and the outer layers of the intestine were gently dissected out. The epithelium was cut longitudinally and pieces about 2 cm long were used for the chambers. Discs of adequate diameter were cut from an acetate sheet and an oblong hole with an area of 0.32 or 0.5 cm^2 was punched into the centre of each disc. The epithelium was glued to the rim of these holes with tissue adhesive (isobutyl-2-cyanoacrylate, Ethicon).

Three complementary approaches were used in this work, following the protocols summarized below: (1) monitoring of the spontaneous potential (V_{tot}) and short-circuit

current (I_{sc}) under different experimental conditions (ion substitutions, or addition of transport inhibitors); (2) recording of intracellular potentials (V_i) and ionic concentrations, also under different experimental conditions, in particular, ion substitutions in the external solutions; and (3) measurement of unidirectional fluxes of sodium, potassium and chloride using, as tracers, ^{22}Na, ^{86}Rb and ^{36}Cl respectively.

Transepithelial electrical parameters

Preparations with an exposed area of 0.32 cm^2 were mounted in Ussing-type chambers and bathed with Ringer's solution (control solution) containing (in mmol l^{-1}): NaCl, 118; KCl, 4.7; $NaHCO_3$, 25; $CaCl_2$, 3.0 (approximately 0.9 mmol l^{-1} free calcium); $MgCl_2$, 1.0; glucose, 5.0; mannitol, 10.0. The composition of this solution was adapted from Ando and Kobayashi (1978). In five animals, anaerobic measurements of pH, P_{CO_2} and bicarbonate concentration in arterial blood using a pK′ of 6.15 and a value of 2.48×10^{-4} mmol l^{-1} Pa^{-1} for α (Severinghaus *et al.* 1956; Boutilier *et al.* 1979) were 7.74±0.014, 2.56±0.21 kPa and 24.5±1.4 mmol l^{-1} respectively. In ion substitution experiments, sodium and potassium were equimolarly replaced by *N*-methyl-D-glucamine (NMG) and chloride was replaced by gluconate. In these solutions, the ionic calcium concentration was measured with a calcium electrode (Diamond Electro-tech Inc, no. 603) and adjusted to 1 mmol l^{-1}. The solutions were kept at a pH of 7.4 by bubbling with a humidified mixture of 95 % O_2 plus 5 % CO_2. The osmolality of all solutions was 290 mosmol kg^{-1}. Electrical continuity between the KCl-saturated solutions, where the current-injecting electrodes (Ag/AgCl) and the voltage-measuring (calomel) electrodes were immersed, and the two half-chambers was made through salt bridges of 3 % agar in control solution. To avoid non-zero junction potentials, all ion replacements were bilateral, with the exception of potassium substitutions. In these experiments, it can be shown that the predicted values (0.2 mV) of the junction potentials can be neglected. Calomel electrodes were regularly manufactured in the laboratory and maintained short-circuited. Before each experiment, the chambers were assembled without the preparation and calomel electrodes differing by less than 0.1 mV were selected. The resistance between the tips of the voltage bridges (G_r) was then measured. An equilibration period of 30–60 min was allowed after mounting the preparation for a stable transepithelial potential to be reached and then the experiments were started under voltage-clamp conditions. The preparation had a conductance comparable to that of the layers of the solution between the tips of the voltage bridges. The total conductance (G_t) of the preparation was then measured and the series-resistance compensation of the voltage-clamp was adjusted so that:

$$I_{sc} = I'\{1 + [G_t/(G_r - G_t)]\}, \quad (1)$$

where I_{sc} is the true short-circuit current and I' is the uncorrected current. For further details see Ferreira *et al.* (1992).

Intracellular potentials and ionic contents

In these experiments, the preparation glued onto the acetate disc was laid on a fine wire mesh with the apical side facing up, and set on a horizontal Ussing-type perfusion

chamber fixed onto an anti-vibration table. The electrodes were mounted on a hydraulic micromanipulator. The baths flowed into both compartments of the chamber by gravity at a rate of $5\,\mathrm{ml\,min^{-1}}$ and two multirotary valves were used to change the solutions. The time for 90 % turnover of the solutions was about 20 s.

Simple microelectrodes were pulled from filamented 1.2 mm o.d. borosilicate glass tubes and filled with $0.5\,\mathrm{mol\,l^{-1}}$ potassium acetate plus $10\,\mathrm{mmol\,l^{-1}}$ potassium chloride solution just before each experiment. Electrodes with resistances between 40 and 90 MΩ were used.

Double-barrelled ion-sensitive microelectrodes were prepared by gluing two pieces of the same glass together (with Standard Araldite). A horizontal Narishige puller was used to twist and pull the microelectrodes. The longer barrel was silanized by vapour treatment with dimethyl dichlorosilane ('simple room temperature method'; Thomas, 1978) for about 1 min and oven-baked at 150 °C for 2 h. The shanks were filled with potassium, sodium or chloride ion exchangers (K-lix Corning 477317; Na-ligand ETH, Fluka 71732; Cl-lix Corning 477913). The back-filling solutions were $100\,\mathrm{mmol\,l^{-1}}$ potassium chloride for potassium and chloride electrodes and $100\,\mathrm{mmol\,l^{-1}}$ sodium chloride for sodium electrodes. Electrodes were kept in dry air and were viable for a few days.

Potassium- and chloride-sensitive microelectrodes were selected by calibration in pure KCl solutions within a concentration range of 10–$100\,\mathrm{mmol\,l^{-1}}$ and had slopes of over 50 mV per decade. Sodium-sensitive microelectrodes were selected by calibration in pure NaCl solutions within a concentration range of 5–$50\,\mathrm{mmol\,l^{-1}}$ and also had slopes over 50 mV per decade. The electrodes were recalibrated during the course of the experiments. For the sodium-sensitive microelectrodes, the calibration solutions contained $50\,\mathrm{mmol\,l^{-1}}$ KCl to take into account the interference of intracellular potassium with sodium readings. Ideally, interference by bicarbonate or other anions with chloride measurements should be determined by taking measurements after removing chloride from the cells. Simple computations showed that, for the concentrations of chloride and bicarbonate in the baths and for the estimated concentrations of these ions inside the cells, interference by bicarbonate could be neglected. Both barrels of the microelectrodes were connected to the electrometers (WPI FD223) by means of silver/silver chloride wires. The signal of the reference electrode was electronically subtracted from the signal of the ion-sensitive electrode and this difference was continuously monitored on a multichannel chart recorder together with the intracellular potential and the transepithelial current under voltage clamp. I_{sc} and V_i, together with direct output from the ion-sensitive channel and from the electronic difference, were digitally converted (12-bit AD converter) and recorded every 2 s for later data processing. The outputs of both amplifiers were adjusted to zero, before each impalement, with the microelectrode dipped in the upper bath.

Ion flux measurements

^{36}Cl, ^{22}Na and ^{86}Rb were used as tracers for chloride, sodium and potassium. Pairs of preparations from the same animal, matched for total conductance, were selected to measure flux in both directions. 7.4×10^4 Bq of the isotope was added to the mucosal side of one of the chambers and to the serosal side of the matched pair. After an equilibration

period of 1 h, the cold chamber was emptied every 20 min; 0.1 ml of the solution from the labelled side of each chamber was sampled at the beginning and end of each experiment.

^{22}Na activity was measured by gamma counting while ^{36}Cl activity was measured by beta counting in Bray's solution. For more details see Coimbra *et al.* (1988). In a number of experiments, ^{36}Cl and ^{22}Na fluxes were measured simultaneously in the same direction. Samples of ^{22}Na were counted in the gamma and beta counters to obtain a correction factor. Fluids collected during the experiments were first counted in the gamma counter and then in the beta counter. Chloride activity was then computed from the beta counts minus the gamma counts multiplied by the correction factor. ^{36}Cl was not detected in the gamma counter.

The following transport inhibitors were used: furosemide (Hoechst, 0.1 mmol l^{-1}); ouabain (Sigma, 0.1 mmol l^{-1}); amiloride, (Merck, Sharp & Dohme, 1.0 mmol l^{-1}); 4,4-diisothiocyano-stilbene 2,2 disulphonic acid (DIDS, Sigma, 0.1 mmol l^{-1}); $BaCl_2$ (3 mmol l^{-1}); acetazolamide (Diamox, Lederle, 1 mmol l^{-1}), H25 (Hoechst, 60 μmol l^{-1}), H74 (Hoechst, 75 μmol l^{-1}), R(+)-butylindazone (Research Biochemical Incorporated, 0.1 mmol l^{-1}) and picrylsulphonic acid (PSA, Sigma, 0.5 mmol l^{-1}). Concentrations between parentheses correspond to the final concentrations in the chambers. Inhibitors were always applied to only one side of the epithelium.

The side of the epithelium corresponding to the lumen of the intestine will be called the mucosal (M) or apical side, while the opposite side will be called the serosal (S) or basolateral side. The expression apparent permeability will be used to designate the ratio between the flux and the concentration gradient of an ion, regardless of the translocation mechanism involved.

Statistical results are presented as means and standard errors of the means (S.E.M.). All statistical tests are *t*-tests (Hald, 1952). The *P* values given correspond to errors of the second kind.

Results

The eel intestine is a single-layer epithelium (Ando and Kobayashi, 1978) which, when mounted in Ussing-type chambers bathed on both sides by a solution with an ionic composition similar to that of the plasma of the animal (see Materials and methods), generates, after a transient period that can last an hour, a spontaneous and stable electrical potential difference (V_{tot}, mucosal side positive) that lasts many hours. The absolute value of this potential depends on the previous salt adaptation of the animal (Ando *et al.* 1975). Under our experimental conditions, overnight salt adaptation was used in only a few experiments to obtain more favourable ratios of net/backfluxes in sodium flux measurements. For pooled results (Fig. 1A), the absolute value of V_{tot} was 2.08±0.11 mV (N=84, serosal side negative). The electrical conductance of the epithelium (G_{tot}, Fig. 1C) was 38.4±1.79 mS cm^{-2} (N=84). The I/V curve of the preparation was linear and the measured short-circuit current (I_{sc}, Fig. 1B), corresponding to the flow of a negative current in the mucosal-to-serosal direction, was 67.5±4.13 μA cm^{-2} (N=154), a high rate of transport.

I_{sc} may be due to a net flow of chloride towards the serosal side, to net flows of sodium or potassium in the opposite direction or to a combination of anionic and cationic flows.

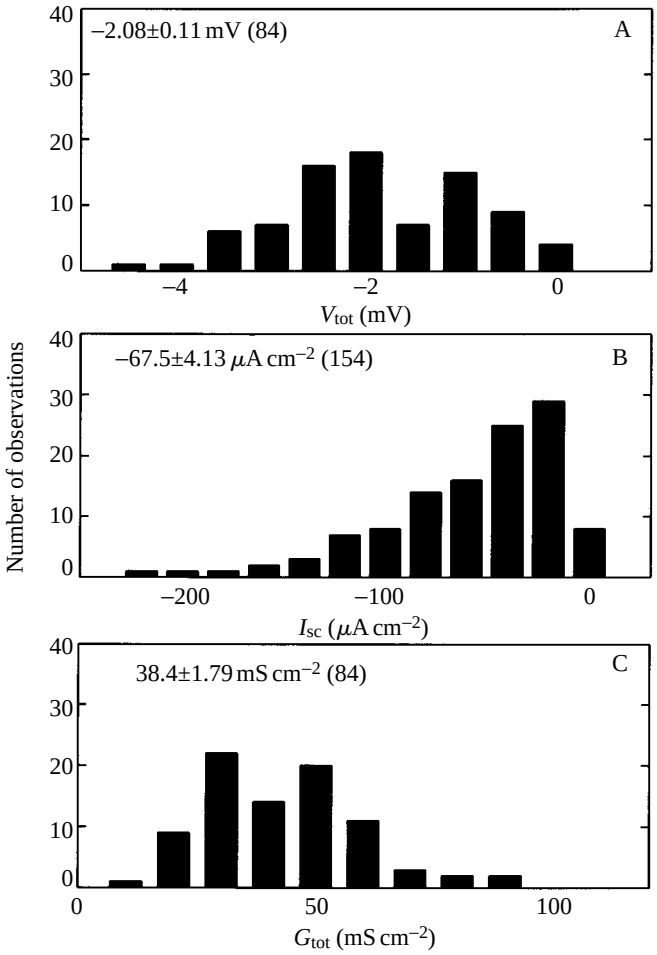

Fig. 1. Histogram of the transepithelial electrical parameters of eel intestine, measured under control conditions, in preparations mounted in Ussing chambers. (A) Transepithelial potential (V_{tot}) in mV; (B) short-circuit current (I_{sc}) in μA cm^{-2}; (C) total conductance (G_{tot}) in mS cm^{-2}. Mean values ± S.E.M. are given in the upper left-hand corner of each panel. Number of values is given in parentheses.

To analyze the nature of this current, its dependence on the ionic composition of the external solution was studied. The current was completely abolished when potassium, sodium or chloride was replaced bilaterally in the external solutions by nominally impermeant ions of the same polarity (Fig. 2A,B,C). In the cases of sodium and chloride replacements (Fig. 2B,C), there were large and slow overshoots of I_{sc} upon removal of either ion, giving rise to large peaks of mucosal-to-serosal positive currents. Reintroduction of control solution in the sodium replacement experiments induced large and slow peaks of negative mucosal-to-serosal currents. Reintroduction of control solution in the chloride replacement experiments (Fig. 2C) did not induce peaks of negative currents and I_{sc} did not recover completely. The unilateral replacements of

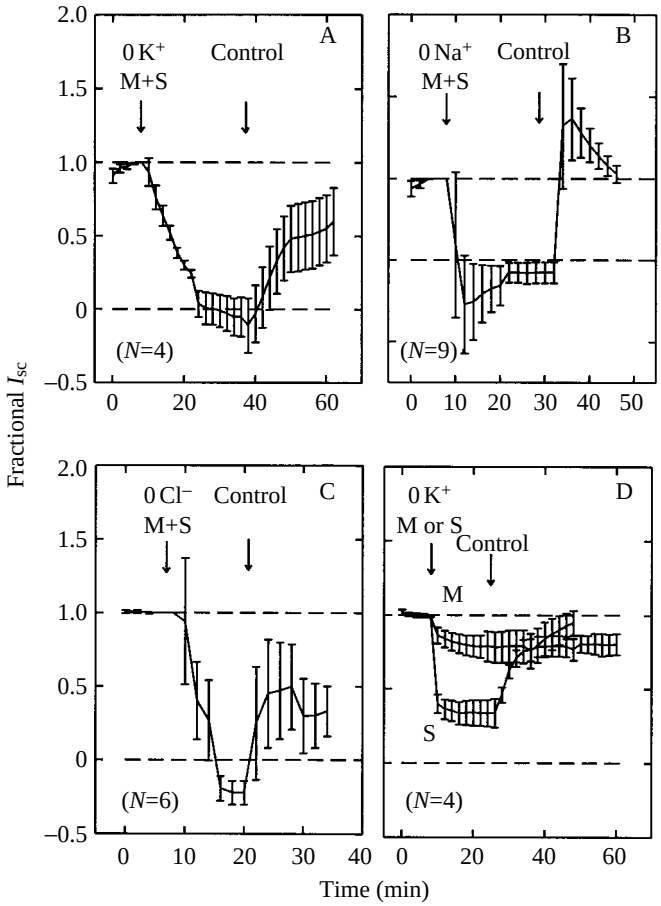

Fig. 2. Time course of the effects of ion substitutions in the external solutions on I_{sc}. The plotted current values are expressed as a fraction of the current measured at the moment when the first substitution was performed. (A) Bilateral substitution of potassium by sodium. (B) Bilateral replacement of sodium by NMG. (C) Bilateral substitution of chloride by gluconate. (D) Unilateral substitution of potassium by sodium on the mucosal (M) or the serosal (S) side. The first arrow signals the moment when the first replacement was performed and the second one the reintroduction of the control solution (recovery). Numbers of experiments are given in parentheses. Mean values are plotted. Error bars correspond to the S.E.M. Values of I_{sc} (mean ± S.E.M.) immediately before first replacement are: 0 Na^+ (both sides) 40.3±8.06 μA cm^{-2}; 0 K^+ (both sides) 55.9±4.2 μA cm^{-2}; 0 Cl^- (both sides) 40.4±7.6 μA cm^{-2}; 0 K^+ (serosa) 84.0±6.9 μA cm^{-2}; 0 K^+ (mucosa) 94.0±22.9 μA cm^{-2}.

sodium or chloride generated such large diffusional currents, in agreement with the open-circuit observations of Ando (1985), that we were unable to measure their effect on I_{sc} with an acceptable precision. The corresponding results are not presented here. Removal of potassium from the mucosal side (Fig. 2D) caused a small inhibition of I_{sc} (around 20 %), whereas removal of the same ion from the serosal side (Fig. 2D) produced an inhibition of around 70 % of the current.

Under strict short-circuit conditions, the mucosal and the serosal compartments have the same composition and are at the same electrical potential; the intracellular compartment can therefore be treated as the cell compartment of an isolated cell. Under these conditions, the intracellular electrical potential (external solutions used as reference) was −33.4±1.08 mV (*N*=59, Fig. 3A) and the concentrations of sodium, potassium and chloride were 31.5±1.3 (*N*=17), 92.4±2.7 (*N*=11) and 54.3±7.7 mmol l^{-1} (*N*=6) respectively (Fig. 3B). From these values and from the intracellular electrical potentials measured in the same cells, the electrochemical potential gradients for the three ions could be computed and were (outside baths used as reference) −74.8±1.2 mV

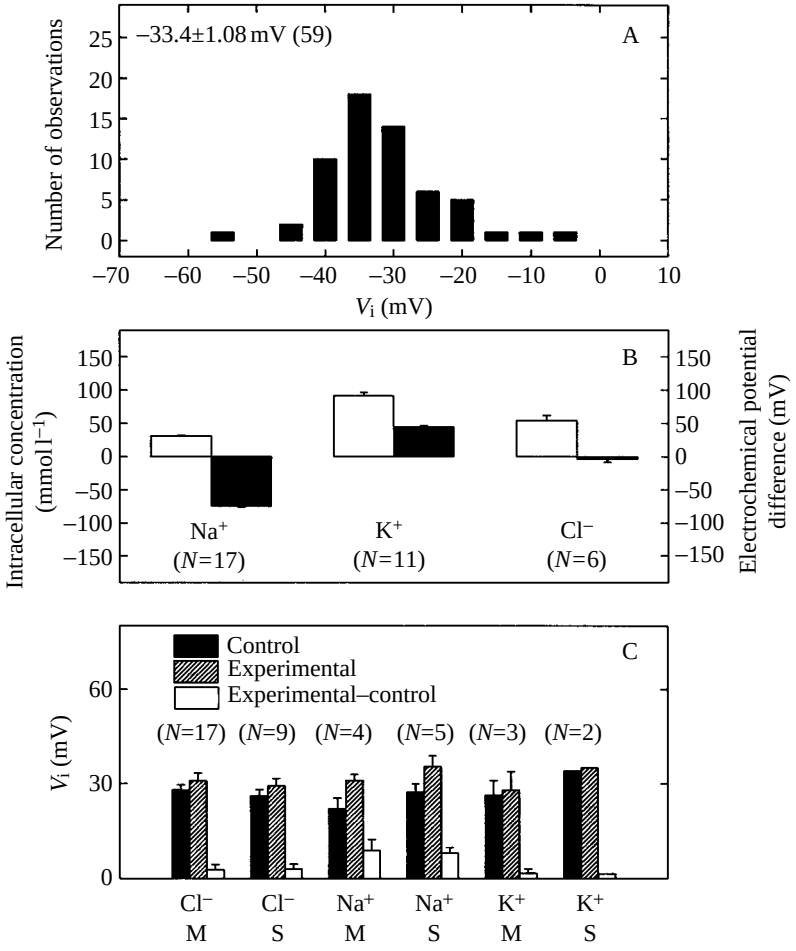

Fig. 3. Measurements of intracellular electrical potentials and ion concentrations. (A) Histogram of the intracellular electrical potentials (V_i) measured with microelectrodes. (B) Intracellular ion concentrations (filled bars) measured with microelectrodes and electrochemical potential gradients (open bars) computed from these values and V_i measured in the same cells. (C) Effect on V_i of unilateral ion replacements (M, mucosal side; S, serosal side). Means and S.E.M. are shown. Numbers of observations (equal to the number of animals) are given in parentheses.

(N=17) for sodium, 43.3±2.4 mV (N=11) for potassium and −4.5±3.00 mV (N=6) for chloride (Fig. 3B). This last value is not statistically different from zero. Thus, there were substantial electrochemical gradients favouring the efflux of potassium from, and the uptake of sodium into, the cell compartment.

The equimolar bilateral replacement of sodium by NMG hyperpolarized the intracellular compartment by 15.0±1.33 mV (N=26), while a similar replacement of potassium had an effect statistically not different from zero (0.29±0.57 mV, N=12) on V_i. Although occasional hyperpolarizations of V_i of up to 9 mV were observed with the equimolar bilateral replacement of chloride by gluconate, the overall result was statistically not different from zero (1.86±1.1 mV, N=14).

The effect on V_i of unilateral ionic substitutions can be seen in Fig. 3C. These results confirm observations with bilateral substitutions, showing that the intracellular electrical potential is only sensitive to sodium replacements in the external solutions.

Unilateral or bilateral ionic replacements in conjunction with intracellular measurements of the electrical potential and of the ionic concentrations can provide some indications of the permeability of the mucosal and serosal barriers to sodium, potassium or chloride. Fig. 4 illustrates the time course of V_i and of the intracellular concentration of chloride $[Cl^-]_i$ when this ion is removed from both sides (Fig. 4A), from the mucosal (Fig. 4B) and from the serosal side (Fig. 4C). The initial efflux rate is much larger across the serosal barrier (0.33 mmol min^{-1}) than across the mucosal barrier (0.016 mmol min^{-1}). These differences in the efflux rates are not reflected in consistent changes of V_i.

Fig. 4D shows that the bilateral replacement of sodium by NMG (first arrow) caused a fall in intracellular sodium concentration with a rate of efflux of 0.34 mmol min^{-1} and a slow hyperpolarization. The change in V_i was reversed when sodium was reintroduced in the mucosal solution (second arrow), but intracellular sodium concentration only rose when the control solution was reintroduced on both sides (third arrow). Removal of sodium from the mucosal side alone (fourth arrow) again caused a hyperpolarization, but did not affect the time course of the intracellular sodium concentration. This observation indicates an important recirculation of sodium across the serosal barrier.

Fig. 4E shows that intracellular potassium concentration falls when potassium is removed from both sides, while V_i remains practically unaffected. Since, in this experiment, the baseline of the intracellular potassium concentration was drifting downwards, it is difficult to estimate the initial rate of efflux. Taking into account the baseline drift, a value of 0.27 mmol min^{-1} was estimated. In most experiments V_i was insensitive to the removal of potassium from the external solutions and $[K^+]_i$ was not visibly altered during the observation period (5–30 min) when potassium was removed unilaterally from the external solutions.

Table 1 reports the values of unidirectional fluxes of sodium, potassium and chloride measured with ^{22}Na, ^{86}Rb and ^{36}Cl. The unidirectional sodium fluxes are very large in both directions, probably as a result of a cation-selective paracellular pathway. To observe a statistically significant net flux for sodium, the preparations in which mucosal-to-serosal and serosal-to-mucosal fluxes were measured had to be matched very precisely

for both I_{sc} and V_{tot}. These experiments are presented as a separate set in the upper part of Table 1. Under short-circuit conditions, there was a net mucosal-to-serosal flux of sodium of 0.89±0.37 nmol cm^{-2} s^{-1}, representing a fraction of 0.73±0.29 of J_{sc} measured in the same preparations but, in terms of charge flow, in the opposite direction. This value is statistically different from zero (P<0.02) but not from 1 (P<0.4). In the same group of experiments, there was a net mucosal-to-serosal flow of chloride of

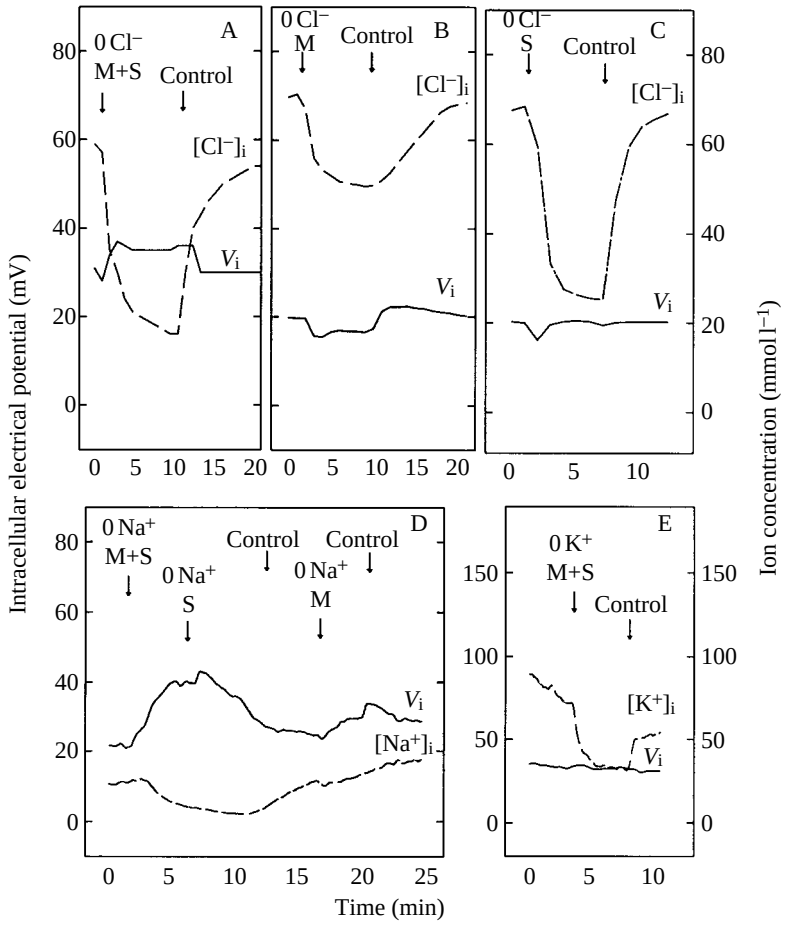

Fig. 4. Time course of changes in intracellular electrical potential (V_i) and ion concentration ($[Cl^-]_i$, $[Na^+]_i$ or $[K^+]_i$) in single experiments in which ion replacements were performed in the bathing solutions. (A) Bilateral chloride substitution. (B) Chloride substitution on the mucosal side. (C) Chloride substitution on the serosal side. In A–C, the first arrow marks the ion substitution and the second arrow marks the return to control conditions. (D) Sodium substitution on both sides (first arrow) followed by reintroduction of the control solution on the mucosal side (second arrow) and on the serosal side (third arrow); after a recovery period, sodium was withdrawn again from the mucosal side (fourth arrow) and later replaced (fifth arrow). (E) Potassium substitution on both sides of the preparation (first arrow) followed by recovery (second arrow). Concentrations are given in mmol l^{-1} and intracellular electrical potentials in mV.

3.02±0.60 nmol cm^{-2} s^{-1}, corresponding to 2.9±0.52 times J_{sc} measured in the same preparations, a value that cannot be distinguished statistically from 2 (P<0.2) or 3 (P<0.1). The middle part of Table 1, corresponding to a larger set of experiments, confirms that there is a net mucosal-to-serosal flow of chloride corresponding to a charge flow of twice the magnitude of I_{sc} and in the same direction. These measurements indicate there is a mucosal-to-serosal net flow of both chloride and sodium ions in a ratio of approximately 2:1. The unidirectional fluxes of potassium (measured with ^{86}Rb) were 0.19±0.013 nmol cm^{-2} s^{-1} (mucosa to serosa) and 0.27±0.011 nmol cm^{-2} s^{-1} (serosa to mucosa), respectively, with the net flux (−0.08±0.016 nmol cm^{-2} s^{-1}) being towards the lumen side, as the sign indicates. As with sodium, the unidirectional fluxes are very large compared with the net fluxes and are 1/30 of the unidirectional sodium fluxes. This is precisely the potassium/sodium concentration ratio in the control solution.

Table 1. *Unidirectional fluxes of sodium, chloride and potassium measured with ^{22}Na, ^{36}Cl and ^{86}Rb under short-circuit conditions*

	J_{Cl}	J_{Na}	J_K	J_{sc}	V_{tot} (mV)
M→S	4.91±0.50	5.73±0.33		1.17±0.06	1.78±0.1
S→M	1.89±0.32	4.84±0.16		1.19±0.07	1.79±0.1
J_{net}	3.02±0.60	0.89±0.37			
J_{net}/J_{sc}	2.9±0.52	0.73±0.29			
N=14					
M→S	4.76±0.34			1.11±0.06	2.05±0.1
S→M	2.41±0.29			1.40±0.11	2.18±0.1
J_{net}	2.35±0.32				
J_{net}/J_{sc}	1.95±0.28				
N=24					
M→S			0.19±0.013	1.39±0.11	6.17±1.3
S→M			0.27±0.011	1.79±0.11	5.61±0.9
J_{net}			–0.08±0.016		
J_{net}/J_{sc}			0.015±0.03		
N=34					

Fluxes are expressed in nmol cm^{-2} s^{-1}.

J_{sc} was obtained by dividing the values of the short-circuit currents expressed in nA cm^{-2} s^{-1} by 96500 C.

All values are expressed as mean ± S.E.M. of the means.

The upper set of values corresponding to 14 experimental periods (five experiments) was selected in such way that mucosal-to-serosal (M→S) and serosal-to-mucosal (S→M) fluxes were measured in paired pieces of epithelium, closely matched for both J_{sc} and V_{tot}. In these experiments, the J_{net}/J_{sc} ratio for chloride is not statistically different from either 3 (P<0.9) or 2 (P<0.2), whereas for sodium it was not different from 1 (P<0.4). The middle set of values corresponds to a larger group of experiments (24 experimental periods) where the paired pieces were less closely matched. The J_{net}/J_{sc} ratio for chloride in these experiments was not statistically different from 2, but was statistically different from either 1 (P≪0.01) or 3 (P≪0.01). The lower set of values corresponds to 34 experimental periods where unidirectional fluxes of potassium were measured. The J_{net}/J_{sc} ratio for potassium was not statistically different from zero (P<0.6).

Fig. 5 reports the effects on I_{sc} of acetazolamide (Diamox) and of a group of transport inhibitors. The values of I_{sc} at any time were divided by the value at the time when the inhibitor was added and the effects when the inhibitor was added to the mucosal (M) or the serosal (S) side were studied separately.

Both furosemide applied from the mucosal side and ouabain applied from the serosal side, at 0.1 mmol l^{-1}, inhibited I_{sc} almost completely (Fig. 5A). Occasionally, furosemide

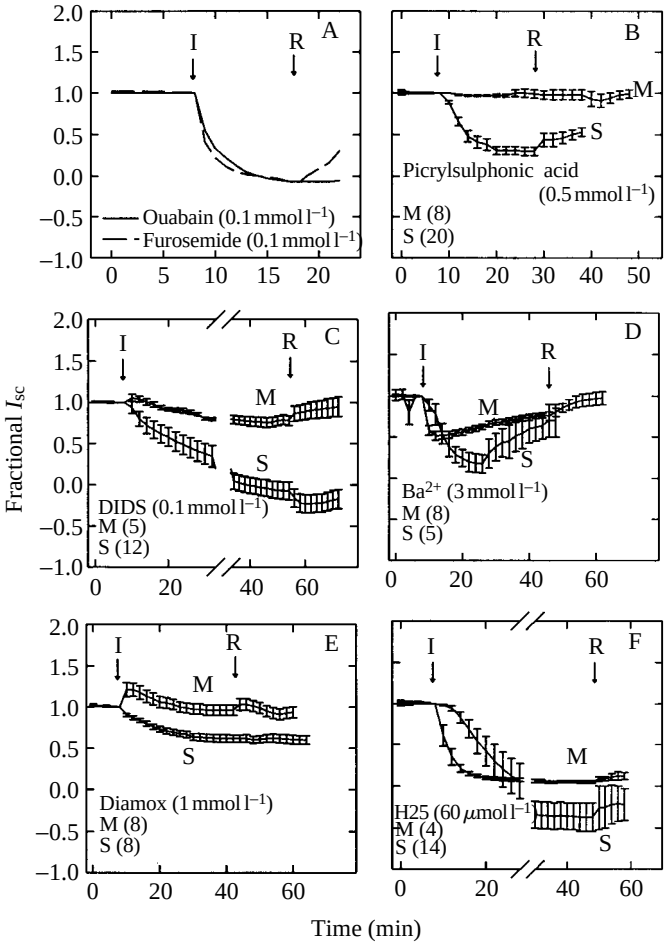

Fig. 5. Time course of the effects of a group of transport inhibitors and Diamox on I_{sc}. Plotted currents are expressed as a fraction of the value of the current at the moment when the inhibitor was added. Two single experiments are plotted in A, whereas in the other panels the continuous lines correspond to the mean values of the number of experiments shown in parentheses. The error bars give the S.E.M. S, serosal side; M, mucosal side. The final concentration for each inhibitor is also given in parentheses. Arrow I indicates the moment when the inhibitor was added and arrow R, the moment when the chambers where washed and filled with control solution. Values of I_{sc} at the moment of adding inhibitor were (mean ± S.E.M. in $\mu A\,cm^{-2}\,s^{-1}$): DIDS, (M) 68.3±12.5, (S) 43.9±10.0; Diamox, (M) 118.0±12.3, (S) 100.0±10.0; barium, (M) 60.7±6.5, (S) 48.3±7.2; picrylsulphonic acid, (M) 96.3±12.5, (S) 90.4±3.18; H25, (M) 267.2±39.2, (S) 36.7±5.9.

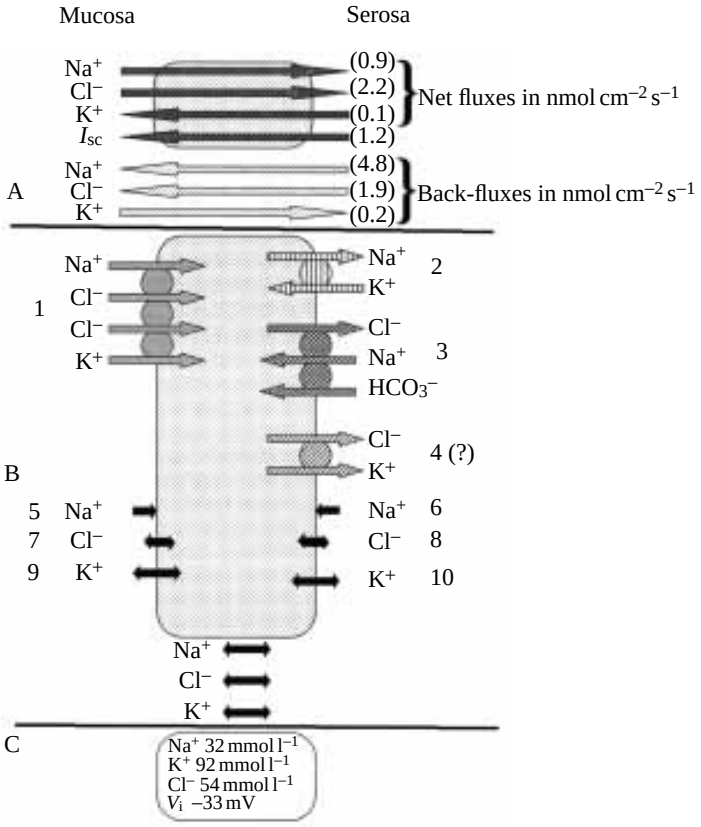

Fig. 6. Pictorial presentation of the main findings. (A) Numerical values (in parentheses) of the ionic fluxes (normalized to an I_{sc} of 1.17 nmol cm^{-2} s^{-1}) measured with radio-isotopes and of the short-circuit current. Since all measurements were performed at zero transepithelial electrical potential difference, the net fluxes (dark arrows) are assumed to be transcellular, while the back-fluxes are assumed to be paracellular. (B) Location of the main transport mechanisms identified through the action of transport inhibitors: 1, inhibited by furosemide; 2, inhibited by ouabain; 3, inhibited by picrylsulphonic acid and DIDS; 4, inhibited by H25. The question mark indicates that, at this stage, there is no clear evidence of the presence of K^+/Cl^- symport since H25 acts from both sides. Black arrows represent uncoupled, conductive fluxes. The conductive permeability to sodium (5, 6) is very low and the permeability to potassium (9, 10) is probably higher than to chloride (7, 8). (C) Intracellular concentrations of sodium, potassium and chloride and intracellular electrical potential under short-circuit conditions.

caused a slight reversal of the current polarity. In 36 experiments, the residual I_{sc} was an average 0.13±0.04 of the control value and there was a current inversion in only six experiments. The effect of furosemide was partially reversible. Both drugs acted with a similar time course (rate constants were 0.51 min^{-1} for ouabain and 0.71 min^{-1} for furosemide).

Picrylsulphonic acid (0.5 mmol l^{-1}, Fig. 5B), an inhibitor of the sodium-dependent bicarbonate/chloride antiport (Madshus and Olsnes, 1987), produced an 80 % inhibition

of I_{sc} when added to the serosal bath. The initial rate constant of current fall was $6.1\,min^{-1}$.

DIDS ($0.1\,mmol\,l^{-1}$, Fig. 5C) was also effective only when added from the serosal side and caused a complete inhibition of I_{sc} with an initial rate constant of $2.64\,min^{-1}$. Occasionally, there was a reversal in polarity of the current, similar to that observed with ouabain or furosemide, and the effect was irreversible.

Barium ($3\,mmol\,l^{-1}$, Fig. 5D) acted from both sides, causing a very fast fall in I_{sc} (rate constants $10.2\,min^{-1}$ from mucosal side and $6.84\,min^{-1}$ from the serosal side). The effect was transient and completely reversible. When added to the serosal side, barium very frequently induced slow oscillations of current (and voltage).

Diamox ($1.0\,mmol\,l^{-1}$, Fig. 5E) inhibited around 40 % of I_{sc} when applied from the serosal side and was ineffective when applied from the mucosal side.

H25 (Hoechst), an inhibitor of the $2Cl^-/Na^+/K^+$ and the K^+/Cl^- symporters (Ellory *et al.* 1990) at $60\,\mu mol\,l^{-1}$ produced, from the serosal side, a very slow inhibition, which started at an initial rate of fall with a rate constant of $1\,min^{-1}$ and accelerated to a value ten times larger than this approximately 5 min after its addition to the serosal bath (Fig. 5F). I_{sc} fell from 49.8±9.53 to -11.71±4.86 $\mu A\,cm^{-2}$ (N=14), the last value being statistically different from zero. The same inhibitor added at the same concentration to the mucosal side induced an immediate fall of I_{sc} from 270±44.28 to 12.1±5.1 $\mu A\,cm^{-2}$ (N=4). The initial rate constant was $15\,min^{-1}$.

Amiloride ($1\,mmol\,l^{-1}$) was ineffective when applied from either side, whereas H74 ($75\,\mu mol\,l^{-1}$) and R(+)-butylindazone ($0.1\,mmol\,l^{-1}$), inhibitors of the K^+/Cl^- symporter (Ellory *et al.* 1990; Garay *et al.* 1988), had no effect on I_{sc} when added to the serosal side.

Table 2. *Steady-state simulation of the effect on* V_i *(in mV) of ion replacements in the external solutions, under short-circuit conditions*

Condition	V_i (experimental) (mV)	V_i (computed) (mV)
Control	–33	–33
Zero Na^+	–48 (15)	–48 (15)
Zero K^+	–33 (0)	–30 (–3)
Zero Cl^-	–35 (2)	–36 (3)
α=8.5; β=2.2		

Zero means that the ion was bilaterally replaced by an impermeant ion of the same polarity and valence (NMG, Na^+ and gluconate, respectively).

The Goldman–Hodgkin–Katz equation for the voltages (see text) was used.

The concentrations of chloride and bicarbonate were lumped. The cell compartment of the epithelium was treated as that of an isolated cell and the permeabilities to sodium (P_{Na}), potassium (P_K) and chloride (P_{Cl}) are the sum of the permeabilities of the two barriers (apical and basolateral) to these ions. With these assumptions, $\alpha=P_K/P_{Na}$ and $\beta=P_{Cl}/P_{Na}$.

Values of V_i (experimental) have been normalized for an average control value of –33 mV.

Differences V_i (control) minus V_i (substitution) are given in parentheses.

Discussion

Fig. 6 reports the main findings of this work, together with a tentative interpretation of their meaning. In Fig. 6A, the values of I_{sc}, of the net fluxes of sodium, potassium and chloride and of the backfluxes of these same ions are given. All values have been normalized to the value of I_{sc} of the upper part of Table 1 ($1.17\,nmol\,cm^{-2}\,s^{-1}$) and the expression 'backfluxes' is applied, for each ion, to the unidirectional fluxes in the direction opposite to that of the corresponding net flux. All fluxes are expressed in $nmol\,cm^{-2}\,s^{-1}$ ($1\,\mu A\,cm^{-2} \approx 10\,pmol\,s^{-1}\,cm^{-2} \approx 0.037\,\mu mol\,h^{-1}\,cm^{-2}$). As described in the Results, the net fluxes of sodium and chloride are approximately one and two times I_{sc} respectively. There was, however, a large variability in these two ratios which, in our experience, cannot be due solely to the fact that the unidirectional fluxes were very large (up to more than four times I_{sc}). If this variability is not due entirely to experimental error, it indicates a variable degree of recirculation of the three ions across the two barriers. The backfluxes are assumed to take place through a hydrophilic paracellular pathway, a reasonable supposition, taking into account their absolute values, and can be used to estimate the permeabilities of the shunt to sodium, potassium and chloride (3.4×10^{-5}, 3.4×10^{-5} and $1.6\times10^{-5}\,cm\,s^{-1}$ respectively). From these estimates, we can predict that under physiological conditions there is absorption of sodium and chloride and secretion of potassium, unless the concentration of this ion is much higher in the lumen of the intestine than in the blood of the animal, in which case there might be potassium reabsorption. An uphill transport of chloride generates a transepithelial electrical potential (serosa negative) which drives sodium and potassium through the moderately cation-selective paracellular pathway. These large shunt permeabilities also account for the high conductance of the preparation and explain the sizes of the gradient-driven fluxes obtained by other authors in open-circuit experiments (Ando, 1983; Ando and Utida, 1986).

In Fig. 6B the likely mechanisms of transport present are identified. The two most effective inhibitors were ouabain (from the serosal side) and furosemide (from the apical side) at $0.1\,mmol\,l^{-1}$ Both drugs suppressed I_{sc} completely (Fig. 5A). The effect of ouabain shows that the charge movements responsible for I_{sc} are completely driven (albeit indirectly) by the sodium pump (transporter 2) and that the slow time course of its effects (initial rate constant=$0.51\,min^{-1}$) reflects the dissipation of the ion gradients that are maintained by the pump operation (Lew *et al.* 1979). The direction of I_{sc} (flow of a positive current towards the mucosal side or of a negative current towards the serosal side), together with the location of the $2Cl^-/Na^+/K^+$ symporter (transporter 1), rule out sodium ions as the main charge carriers. Nevertheless, the intracellular concentrations of sodium and potassium (Fig. 6C) measured with ion-sensitive microelectrodes can be explained by the operation of the sodium pump.

The black arrows (translocators 5–10) represent uncoupled, conductive fluxes, the so called 'diffusional fluxes'. In the case of the paracellular pathway, they presumably correspond to truly diffusional movements through poorly cation-selective water pathways, while in the case of transcellular movements they are probably translocations through low-affinity specific hydrophilic channels. The sizes of these arrows are a semi-

quantitative indication of their relative corresponding permeability (channel permeability × number of channels per unit area).

As shown in Fig. 5A, furosemide added to the mucosal side inhibited I_{sc} almost completely and without a current reversal. This effect implies that the Na^+ pump is fed exclusively through $2Cl^-/Na^+/K^+$ symport (transporter 1 of Fig. 6). This observation has two implications. (1) The parallel conductive pathway for sodium across the apical barrier is negligible; that is, the diffusional permeability to sodium (Fig. 6, transporter 5) of this barrier is (relatively) very small, otherwise there would have been an inversion of the current direction after the furosemide inhibition. (2) To explain a net transcellular charge flow corresponding to a negative current in the mucosal to serosal direction, we have to postulate a large, conductive potassium recirculation across the apical barrier. Such a model is compatible with our experimental results and in particular with the values of V_i measured under conditions in which sodium, potassium or chloride was equimolarly replaced by impermeant univalent ions of the same polarity.

Under short-circuit conditions, and with the preparation bathed on both sides by the same solution, the intracellular compartment of the epithelium can be treated as if it were the cytoplasm of an isolated cell. The intracellular electrical potential V_i is then given by (Hodgkin and Katz, 1949; Lew *et al.* 1979):

$$V_i = (\boldsymbol{RT}/F)\log_e[(V_iY + J_P)/(V_iX + J_p)], \quad (2)$$

where $\boldsymbol{R}$ (8.315 J degree^{-1} mol^{-1}) is the ideal gas constant, T (≈298 K) is the absolute temperature, F (96500 C mol^{-1}) is the Faraday constant, J_P (V mol cm^{-1}) is the net cation transport rate across the pump multiplied by $\boldsymbol{RT}/F$ and divided by the sodium permeability (responsible for the electrogenicity of the pump, see Lew *et al.* 1979), and X and Y are given by the expressions:

$$X = [Na^+]_i + \alpha[K^+]_i + \beta[Cl^-]_e, \quad (3)$$

$$Y = [Na^+]_e + \alpha[K^+]_e + \beta[Cl^-]_i. \quad (4)$$

In these expressions, i and e designate the intracellular and the extracellular compartments, respectively, and α and β are the overall, lumped (mucosal+serosal) relative permeabilities of the cell membrane to potassium and chloride, in relation to the sodium permeability. Instead of the chloride concentrations, we used the lumped concentrations of chloride and bicarbonate. In our experience, the direct contribution of the pump operation to I_{sc} (through J_P) can be neglected because the addition of ouabain did not produce an immediate sharp fall in current as seen in other systems (Lew *et al.* 1979). Four equations similar to equation 1 can be written, corresponding to the control conditions and to situations in which the external concentrations of sodium, potassium or chloride are set at zero. On the basis of the experiments with ion-sensitive microelectrodes, the intracellular concentrations of sodium or chloride were assumed to fall to zero when the same ion was removed from the external solutions. Also, in agreement with our microelectrode studies, the intracellular potassium concentration was assumed to fall to 40 % of the control value. This assumption takes into account the low rate of fall of intracellular potassium concentration and the duration of the experiments.

With these assumptions, and after inserting appropriate values of α and β, V_i could be computed under control conditions and when sodium, potassium or chloride was replaced by impermeant ions of the same charge. As shown in Fig. 3 the control value of V_i was -33.4 ± 1.08 mV (N=59). The changes in V_i produced by bilaterally replacing sodium, potassium or chloride by impermeant ions in the external solutions were 14 ± 1.35 mV (N=26), 0.29 ± 0.57 mV (N=12) and -1.86 ± 1.39 mV (N=14), respectively, negative values corresponding to depolarizations. A comparison between experimental and computed values is given in Table 2; values of 8.5 and 2.2 were used for α and β respectively. The fit obtained is within experimental error. We can thus assume that the conductive permeability of the two lumped barriers to potassium (Fig. 6, translocators 9 and 10) is much larger than the permeability to the other two ions. The bilateral effect of barium (Fig. 5D) shows that this high permeability is not confined to one of the barriers. The initial rate constant of the fall in I_{sc} induced by barium from the mucosal side is relatively large ($10.5\,min^{-1}$), suggesting the occlusion of conductive potassium channels (Nagel, 1979; Nielsen, 1979). The effect from the serosal side is initially slower (rate constant $6.8\,min^{-1}$), but the curve (Fig. 5D) shows an inflection to be expected from the delay introduced by a large unstirred layer.

The efflux rates of chloride upon removal of this ion from the external solutions indicate a high 'apparent' permeability of both barriers to this ion, the serosal barrier being 20 times more permeable. At present, we are unable to estimate the fraction of this permeability that is conductive, but the ion substitution experiments provide indirect evidence that it is not negligible. The effects of bilateral ion replacements of sodium or chloride (Fig. 2B,C) must be due to the large ionic shifts between the intracellular and the external compartments observed in the experiments with ion-sensitive microelectrodes reported above (see Fig. 4A–D). The transients recorded with ion-sensitive microelectrodes showed that, during these experiments, there is a loss of sodium and chloride from the cell compartment. Since the conductive permeability of the apical barrier to sodium must be (relatively) very small, most of the sodium must leak out across the serosal barrier. To account for the large current overshoots detected in the external circuit, there must be equal currents across the apical barrier due to potassium uptake and/or chloride loss, determined in part by the cell hyperpolarization. Movements in the opposite direction must take place when the control solution is reintroduced into the chambers.

The transient currents across the serosal barrier may involve displacements of three ions. Since we know already that there is an appreciable conductive permeability to potassium in the mucosal barrier, and since the overall relative permeability of chloride (Fig. 6, transporters 7 and 8) is twice that of sodium, it is reasonable to postulate a non-negligible serosal permeability to chloride. However, this permeability does not explain the large net flux of chloride across the serosal barrier. In principle, this flux could occur as a result of three possible mechanisms: diffusion through conductive anionic channels (transporter 8), requiring an electrochemical gradient outwards; K^+/Cl^+ symport (transporter 4), driven by the potassium electrochemical gradient outwards; Cl^-/bicarbonate antiport, sodium-dependent (transporter 3) or otherwise. The negligible electrochemical gradients for chloride between the cell compartment and the outside

compartments, the large transepithelial fluxes of this ion and the very small dependence of V_i on external chloride imply that most chloride movements across the two barriers are coupled to those of other ions (sodium and potassium across the apical barrier, potassium and/or bicarbonate+sodium across the serosal barrier). This being so, one should expect the diffusive permeability to chloride, of both barriers, to be relatively small compared with the overall 'apparent' permeability.

The effect of Diamox applied from the serosal side implies that the intracellular supply or removal of bicarbonate is partially rate-limiting for current generation, either because transmembrane bicarbonate movements are tightly coupled to the movements of an ion involved in current generation or through intracellular pH regulation.

The presence of a serosal K^+/Cl^- symport was proposed for the thick ascending limb of the Henle's loop (Greger and Schlatter, 1983) on the basis of electrophysiological arguments, but was not confirmed by subsequent mathematical simulations (Fernandes and Ferreira, 1991). Of the inhibitors of human red cell K^+/Cl^- symport (H25, H74; Ellory *et al.* 1990, and R(+)-butylindazone; Garay *et al.* 1988) only H25 was effective in our experimental situations. Since H25 acts on $2Cl^-/Na^+/K^+$ symport with an affinity three orders of magnitude greater than the affinity for K^+/Cl^- symport, we cannot rule out the possibility that the drug reached the apical barrier in effective concentrations, a mechanism that would explain the delay of the effect. From our results, we cannot exclude the hypothesis that H25 does not have a site of action different from that of furosemide since it induces an initial rate of fall of I_{sc} that is more than ten times larger than that of furosemide. We have to conclude that there is no compelling evidence for the presence of K^+/Cl^- symport in the basolateral barrier (Fig. 6, transporter 3).

We lack any direct evidence of substantial, conductive sodium fluxes across either barrier (Fig. 6, transporters 5 and 6). The intracellular concentration of sodium fell at a rate of $0.34\,mmol\,min^{-1}$ when sodium was replaced bilaterally by NMG (Fig. 4D); unilateral replacements showed that the efflux across the serosal barrier was much larger than across the apical barrier, an observation that suggests a substantial recirculation of sodium across the serosal barrier. The most likely translocating mechanism for this recirculation, besides the sodium pump, is the sodium-dependent anion shuttle (Fig. 6B, transporter 3).The effects of DIDS and picrylsulphonic acid applied from the serosal side suggest the presence of a sodium-dependent anion shuttle located at the serosal barrier (Madshus and Olsnes, 1987), which might explain, by uncovering a large recirculation of sodium across this barrier, the rapid efflux of sodium from the cell compartment when this ion is replaced in the serosal side. However, such recirculation could not alone explain the large variability in J_{Na}/J_{sc} ratios reported in this work.

DIDS is a known irreversible inhibitor of the chloride/bicarbonate anionic shuttle (Cabantchik and Rothstein, 1972) but also inhibits the sodium-dependent chloride/bicarbonate exchange (Deitmer and Schlue, 1987). The effect of DIDS confirms the observations of Ando (1990) and may indicate that there is an anion exchanger in the serosal barrier (Cl^-/bicarbonate, for instance) or that the drug blocks chloride channels. We could not detect a change in epithelial conductance after the serosal application of DIDS. The first mechanism seems more likely since picrylsulphonic acid had a similar effect. This explanation also fits the observations of Schettino *et al.* (1992), who showed

that, in the absence of serosal sodium, I_{sc} became bicarbonate-independent. However, the initial rate constants of the DIDS inhibition ($2.7\,min^{-1}$) and of the picrylsulphonic acid inhibition ($6.1\,min^{-1}$) were much larger than those of ouabain or furosemide, a result to be expected only if the sodium-dependent anionic shuttle contributed directly to the current generation. The presence of a $Na^+/nHCO_3^-$ symport in the serosal barrier, also sensitive to DIDS (Thomas, 1988), would load the cells with bicarbonate and translocate chloride into the serosal compartment. The bicarbonate might be titrated in part by protons generated by cell metabolism. How well this mechanism could regulate intracellular pH cannot be assessed at present. Uptake of protons could take place across the apical barrier by H^+/Na^+ exchange, driven by the relatively high pH that might result from bicarbonate uptake across the serosal barrier, the overall result being an alkalization of the mucosal compartment and an acidification of the serosal compartment. This hypothesis is excluded by the lack of an effect of amiloride at $1\,mmol\,l^{-1}$, added to the apical side. Bilateral or unilateral replacement of sodium by NMG caused an intracellular hyperpolarization (Fig. 4D). As shown above, this result can be obtained with much larger conductive permeabilities to chloride and potassium. However, we cannot exclude sodium recirculation across the apical barrier but, should it exist, it must take place against an electrochemical gradient of 75 mV, that is by a coupling mechanism to movements of potassium, protons or bicarbonate.

Replacement of potassium in the solutions bathing both sides of the preparation caused complete inhibition of I_{sc} with very little effect on V_i. As shown above, simple steady-state modelling, based on the Goldman–Hodgkin–Katz equation (Hodgkin and Katz, 1949), demonstrates that these effects are entirely predictable. The small inhibition observed when potassium was replaced by sodium on the mucosal side is not, in itself, evidence that a $2Cl^-/Na^+/K^+$ transporter is not present in the apical barrier, because this barrier is highly folded and must thus retain a large unstirred layer. In addition, sodium may replace potassium and thus sustain I_{sc} and also, as observed by Ando (1983), water transport. The almost complete inhibition of I_{sc} caused by the removal of potassium from the serosal bath is probably largely due to the inhibition of the sodium pump. The incomplete inhibition observed cannot be explained with any degree of certainty, unless the net fluxes for the main ions transported are measured simultaneously. It may, at least in part, be due to the recirculation of potassium across the basolateral barrier. The removal of a transepithelial net flux of potassium towards the mucosal compartment cannot be the explanation, because it is less then 10 % of I_{sc}.

I_{sc} could not be maintained when sodium, chloride or potassium was bilaterally replaced by nominally impermeant ions of the same charge. The simplest interpretation of these results is that, at some stage, the fluxes of the three ions are tightly coupled but, in view of the flux measurements, the tightness of this coupling is not confirmed. The effects on I_{sc} of unilateral replacements of sodium or chloride could not be characterized because they were largely masked by diffusional currents, probably taking place through a shunt pathway. Unilateral replacements were studied under open-circuit conditions by Ando (1983), who showed that water transport was maintained when potassium replaced sodium on the mucosal side, was inhibited when the replacement ion was choline or Tris, and was partially inhibited when sodium was substituted by potassium on the serosal side.

The same author showed a clear dependence of the mucosa-to-serosa net flux of chloride on mucosal potassium concentration as well as a dependence of water transport in the same direction on the mucosal sodium concentration and a linear correlation between the net chloride fluxes and the net water flux. It should be noted that these results were obtained under open-circuit conditions and in a different species of eel from the current study.

The results obtained with the bilateral ionic substitutions of sodium, potassium or chloride, together with the effect of furosemide added to the apical side, provide good support for the hypothesis that there is $2Cl^-/Na^+/K^+$ symport (Ando and Utida, 1986) in the apical barrier. If it is present, it should explain the weak effect of the replacement of potassium by sodium on the apical side. Can sodium replace potassium? In the thick ascending limb of the Henle's loop, this is not the case (Greger and Schlatter, 1981). We still lack detailed kinetic and molecular information about the modes of operation of the furosemide sensitive translocator(s?).

We acknowledge the technical support of Mr U. F. Santos. P.M. is a fellow of JNICT (Fellowship BD/2140/92-ID).

References

ANDO, M. (1975). Intestinal water transport and chloride pump in relation to sea-water adaptation of the eel, *Anguilla japonica*. *Comp. Biochem. Physiol.* **52**A, 229–233.

ANDO, M. (1980). Chloride-dependent sodium and water transport in the seawater eel intestine. *J. comp. Physiol*. **138**, 87–91.

ANDO, M. (1981). Effects of ouabain on chloride movements across the seawater eel intestine. *J. comp. Physiol.* **145**, 73–79.

ANDO, M. (1983). Potassium-dependent chloride and water transport across the seawater eel intestine. *J. Membr. Biol.* **73**, 125–130.

ANDO, M. (1985). Relationship between coupled Na^+–K^+–Cl^- transport and water absorption across the seawater intestine. *J. comp. Physiol.* **155**, 311–317.

ANDO, M. (1990). Effects of bicarbonate on salt and water transport across the intestine of the see water eel. *J. exp. Biol*. **150**, 367–379.

ANDO, M. AND KOBAYASHI, M. (1978). Effects of stripping of the outer layers of the eel intestine on salt and water transport. *Comp. Biochem. Physiol.* **61**A, 497–501.

ANDO, M. AND UTIDA, S. (1986). Effects of diuretics on sodium, potassium, chloride and water transport across the seawater eel intestine. *Zool. Sci*. **3**, 605–612.

ANDO, M., UTIDA, S. AND NAGAHAMA, H. (1974). Active transport of chloride in eel intestine with special reference to sea-water adaptation. *Comp. Biochem. Physiol.* **51**A, 27–32.

ANDO, M., UTIDA, S. AND NAGAHAMA, H. (1975). Active transport of chloride in eel intestine with special reference to sea water adaptation. *Comp. Biochem. Physiol*. **51**A, 27–32.

BOUTILIER, R. G., RANDALL, D. J., SHELTON, G. AND TOEWS, D. P. (1979). Acid–base relationships in the blood of the toad *Bufo marinus*. I. The effects of environmental CO_2. *J. exp. Biol.* **82**, 331–344.

CABANTCHIK, Z. I. AND ROTHSTEIN, A. (1972). The nature of the membrane sites controlling anion permeability of human red blood cells as determined by studies with disulfonic stilbene derivatives. *J. Membr. Biol*. **10**, 215–255.

COIMBRA, J., MACHADO, J., FERNANDES, P. L., FERREIRA, H. G. AND FERREIRA, K. G. (1988). Electrophysiology of the mantle of *Anodonta cygnea*. *J. exp. Biol*. **140**, 65–88.

DEITMER, J. W. AND SCHLUE, W. R. (1987). The regulation of intracellular pH by identified glial cells and neurones in the central nervous system of the leech. *J. Physiol., Lond.* **388**, 261–283.

ELLORY, J. C., HALL, A. C., ODY, S. O., ENGLERT, H. C., MANIA, D. AND LANG, H.-J. (1990). Selective inhibitors of the KCl cotransport in human red cells. *FEBS Lett.* **262**, 215–218.

FERNANDES, P. L. AND FERREIRA, H. G. (1991). A mathematical model of rabbit cortical thick ascending limb of the Henle´s loop. *Biochim. biophys. Acta* **1064**, 111–123.

FERREIRA, K. T. G., FERNANDES, P. L. AND FERREIRA, H. G. (1992). Ion transport across the epithelium of the rabbit caecum. *Biochim. biophys. Acta* **1175**, 27–36.

FIELD, M., KARNAKY, K. J., JR, SMITH, P. L., BOLTON, J. E. AND KINTER, W. B. (1978). Ion transport across the isolated intestinal mucosa of the winter flounder, *Pseudopleuronectes americanus*. I. Functional and structural properties of cellular and paracellular pathways for Na and Cl. *J. Membr. Biol.* **41**, 265–293.

GARAY, R. P., NAZARET, C., HANNAERT, P. A., CRAGOE, E. J. AND JR, (1988). Demonstration of a [K^+, Cl^-]-cotransport system in human red blood cells by its sensitivity to [(dihydroindenyl)oxy]alkanoic acids: regulation of cell swelling and distinction from bumetanide-sensitive [Na^+, K^+, Cl^-] cotransport system. *Molec. Pharmac.* **33**, 696–701.

GREGER, R. AND SCHLATTER, E. (1981). Presence of luminal K^+, a prequisite for active NaCl transport in the cortical thick ascending of Henle's lop of rabbit kidney. *Pflügers Arch.* **392**, 92 – 94.

GREGER, R. AND SCHLATTER, E. (1983). Properties of the basolateral membrane of the cortical thick ascending limb of Henle's lop of rabbit kidney. *Pflügers Arch.* **396**, 325–334.

HALD, A. (1952). *Statistical Theory with Engineering Applications*. New York:John Wiley and Sons, Inc. pp. 391–394.

HODGKIN, A. L. AND KATZ, B. (1949). The effect of sodium ions on the electrical activity of the giant axon of the squid. *J. Physiol., Lond.* **108**, 37–77.

LEW, V. L., FERREIRA, H. G. AND MOURA, T. (1979). The behaviour of transporting epithelial cells. *Proc. R. Soc. Lond. B* **206**, 53–83.

MADSHUS, I. H. AND OLSNES, S. (1987). Selective inhibition of sodium-linked and sodium-independent bicarbonate/chloride antiport in vero cells. *J. biol. Chem.* **262**, 7486–7491.

MUSCH, M. W., ORELANA, S. A., KIMBERG, L. S., FIELD, M., HALM, D. R., KRASNY, E. J. AND FRIZELL, R. A. (1982). Na^+–K^+–Cl^- cotransport in the intestine of a marine teleost. *Nature* **300**, 351–353.

NAGEL, W. (1979). Inhibition of potassium conductance by barium in frog skin epithelium. *Biochim. biophys. Acta* **552**, 346–357.

NIELSEN, R. (1979). A 3–2 coupling of the Na–K pump responsible for the transepithelial Na transport in frog skin disclosed by the effect of barium. *Acta physiol. scand.* **107**, 189–191.

PALFREY, H. C. AND RAO, M. C. (1983). Na/K/Cl co-transport and its regulation. *J. exp. Biol.* **106**, 43–54.

SCHETTINO, T., TRISCHITTA, F., DENARO, M. G., FAGGIO, C. AND FUCILE, I. (1992). Requirement of HCO_3^- for Cl^--absorption in seawater-adapted eel intestine. *Pflügers Arch.* **421**, 146–154.

SEVERINGHAUS, J. W., STUPFEL, M. AND BRADLEY, A. F. (1956). Variations of serum carbonic acid pK′ with pH and temperature *J. appl. Physiol.* **9**, 197–200.

THOMAS, R. C. (1978). *Ion Sensitive Intracellular Microelectrodes. How to Make and Use Them*. London: Academic Press. pp. 64–65.

THOMAS, R. C. (1988). Summary. In *Proton Passage across Cell Membranes* (ed. G. Bock and J. Marsh), pp. 254–255. New York: John Wiley and Sons.